DOI 10.1007/s10812-019-00796-3
Journal of Applied Spectroscopy, Vol. 86, No. 1, March, 2019 (Russian Original Vol. 86, No. 1, January–February, 2019)

STUDY OF THE INTERACTION OF QUERCETIN AND TAXIFOLIN WITH β-LACTOGLOBULIN BY FLUORESCENCE SPECTROSCOPY AND MOLECULAR DYNAMICS SIMULATION

Fatemeh S. Mohseni-Shahri

UDC 535.372

The interaction between quercetin and taxifolin with β-lactoglobulin (BLG) was investigated via various methods, including fluorescence spectroscopy, molecular docking and molecular dynamics (MD) simulation. The results have demonstrated that quercetin binds BLG with an affinity higher than that of taxifolin, which is attributed to the nonplanar C-ring and steric hindrance effect in taxifolin. The synchronous fluorescence spectra shows that quercetin and taxifolin do not induce conformational changes of BLG. Molecular docking studies have demonstrated that several amino acids are involved in stabilizing the interaction. Analysis of the MD simulation trajectories shows that the root mean square deviation (RMSD) of various systems reaches equilibrium. Time evolution of the radius of gyration shows as well that BLG and BLG-flavonoid complexes are stable within 5 ns. In addition, analyzing the RMS fluctuations, one can suggest that the structure of the ligand binding site remains rigid during the simulation. The secondary structure of BLG is preserved upon interaction with these flavonoids.

Keywords: *β-lactoglobulin, flavonoid, fluorescence quenching, molecular dynamics simulation.*

Introduction. Lipocalins are small proteins with the capacity to transfer and bind small hydrophobic ligands [1, 2]. The core structure of these proteins includes an eight-stranded antiparallel β-barrels that clarifies an internal cavity for binding the ligands. β-Lactoglobulin (BLG), the major whey protein in cow milk, consists of 162 amino acids with 18.4 kDa of molecular weight [3, 4]. It is popular in our diet and has valuable functional properties. Its ability to bind to a variety of molecules, such as fatty acids, retinol, β-carotene, phospholipids, vitamin D, polyphenolic compounds, and folic acid, is well known [5–11].

Flavonoids are biologically polyphenolic components found in vegetables with broad biological activities and important therapeutic applications, including anticancer, antitumor, anti-inflammatory, antioxidant, and anticoagulant properties [12, 13]. The delivery of flavonoids and their metabolites is poorly understood. The interaction of flavonoids and a transport protein such as BLG could be an invaluable agent to control their transport to biological sites.

Quercetin (3,5,7,3′,4′-pentahydroxyflavone) (Scheme 1a) is one of the most abundant flavonoids in the human diet. Quercetin is well known to have a strong metal ion chelating capacity and antioxidant behavior; hence, it has a variety of biochemical and biological effects, including antioxidative, free radical scavenging, antitumour, and anti-inflammatory and cardioprotective activities [14, 15]. It exists in many common foods and drinks such as tea, onions, olives, beer, and red wine. Another polyphenol flavonoid, taxifolin (3,3′,4′,5,7-pentahydroxyflavanone) (Scheme 1b) is principally found in many citrus fruits, especially orange and grapefruit [16].

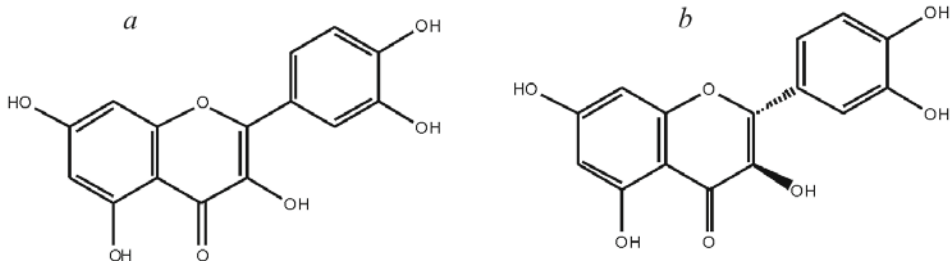

Scheme 1. Chemical structures of (a) quercetin and (b) taxifolin.

Department of Chemistry, Bandar Abbas Branch, Islamic Azad University, Bandar Abbas 7915893144, Iran, email: fmohsenishahri@gmail.com. Abstract of article is published in Zhurnal Prikladnoi Spektroskopii, Vol. 86, No. 1, p. 157, January–February, 2019.

Because of the low bioavailability and poor water solubility of flavonoids caused by their hydrophobic ring structure, the clinical application of them is limited. In addition, an important physicochemical property of BLG is its ability to bind to several physiological ligands. So, BLG can be employed as a depot and transport protein, particularly for molecules with low water solubility. Since the efficacy of milk proteins as carriers for flavonoids has been confirmed by Bohin et al. [17], and finding new bioactive ligand molecules of BLG is of pharmacological and biotechnological significance, it is essential to have a better understanding of molecular identification properties of BLG. BLG shows considerable resistance against both simulated duodenal and gastric digestion. That is why it appears to be an appropriate candidate for the protection and safe delivery of pH sensitive drugs in stomach. The high stability of BLG under acidic condition guarantees the low delivery of hydrophobic ligands in acidic condition of stomach. In this paper, we investigated the interaction between BLG and flavonoids in detail by the spectroscopic and molecular dynamics simulation method under simulated physiological condition.

Materials and Methods. BLG (B form, purity >90%) was purchased from Sigma Aldrich and used without further purification. The two flavonoids including quercetin and taxifolin were purchased from Sigma Aldrich (St. Louis, USA) and used as received. The other chemicals, such as phosphate buffer and ethanol, were all of analytical purity and used without further purification. Double distilled water was used as a solvent throughout the experiment. The BLG stock solution was made by dissolving in 50 mM phosphate buffer at pH 7.4 to obtain the concentration of 100 μM. The BLG concentrations in the solution were determined spectrophotometrically at 278 nm using a molar absorption coefficient of $\varepsilon = 17{,}600\ M^{-1} \times cm^{-1}$ [18]. Fresh stock solutions of natural flavonoid (1 mM) in phosphate buffer were also prepared.

Fluorescence spectra were recorded on a Hitachi MPF-4 spectrofluorimeter (Japan) in a 1-cm path length quartz cell with excitation and emission wavelengths of 290 and 300–500 nm, respectively, at 298 K. The width of the excitation and emission bands was 5 nm. The concentration of BLG was 10 μM, and the concentration of quercetin and taxifolin varied from 0 to 30 μM with a step of 2.0 μM.

The synchronous fluorescence spectra were obtained using simultaneous scanning of the excitation and emission monochromators; they showed only tyrosine (Tyr) and tryptophan (Trp) residues of BLG, when the wavelength interval was 15 and 60 nm, respectively.

Molecular docking has significantly contributed to the elucidation of the mechanism of binding between the protein and ligand. Docking was performed by an ArgusLab 4.0.1 molecular docking program [19]. The crystal structure of BLG (PDB ID: 3NPO) was downloaded from the Brookhaven Protein Data Bank (http://www.rcsb.org/pdb). The water molecules in the used pdb file are not structural; thus, all water molecules were removed from the protein file. The 3D structures of quercetin and taxifolin were made using VEGA ZZ 3.0.1. The geometry of flavonoids was optimized by the density functional theory (DFT) (B3LYP/6-31G) method using Gamess software [20]. The whole protein was taken as a potential binding site, and the blind docking approach was used. For the docking calculations, a core scoring method in ArgusLab was employed, with 0.4 Å grid resolution and maximum 200 candidate poses. In the docking routine, it is assumed that the structure of BLG remains rigid and all the torsional bonds of the flavonoids are set free (flexible docking). The core scoring function ranked the docked conformations basing on their free binding energy. The conformer of each flavonoid-BLG complex with the lowest binding energy was used for further analyses.

The lowest free binding energy conformation of each complex was considered as the initial conformation for the MD studies. All calculations were carried out by Gromacs software version 4.5.4 (University of Groningen, The Netherlands) and the GROMOS96 43a1force field [21]. Since quercetin and taxifolin potential parameters are not defined in the Gromacs software, a PRODRG web server was used to assign these parameters in the framework of the GROMOS force field [22]. Partial atomic charges of the flavonoids were optimized by using the density functional theory (DFT) (B3LYP/6-31G (d)) method using Gamess software [20]. The complex was located in the cubic box with the periodic boundary conditions. The box volume was 274.62 nm^3 ($6.5 \times 6.5 \times 6.5\ nm^3$), and the minimum distance between the protein surface and the simulation box was 1.0 nm. The box filled with extended simple point charge (SPC), water molecules [23], and the solvated systems were neutralized by adding sodium ions (Na^+). Energy minimization was performed using the steepest descent method for 8 ps. Then, the system was equilibrated at the temperature of 300 K. Finally, a 20 ns MD simulation was carried out at 1 bar and 300 K. A Berendsen thermostat at 300 K [24], as well as the PME algorithm were used for each component of the systems to evaluate the electrostatic interactions. In this algorithm, every atom interacts with all other atoms in the simulation box and with all of their images in an infinite array of periodic cells; so, satisfactory results are gained from the electrostatic interactions [25]. The equation of motions was integrated by the leap-frog algorithm with the 2 fs time step. The atomic coordinates were recorded to the trajectory file every 0.5 ps for later analysis. Finally, an all-bond constraint was used to prevent the ligand from drifting in MD.

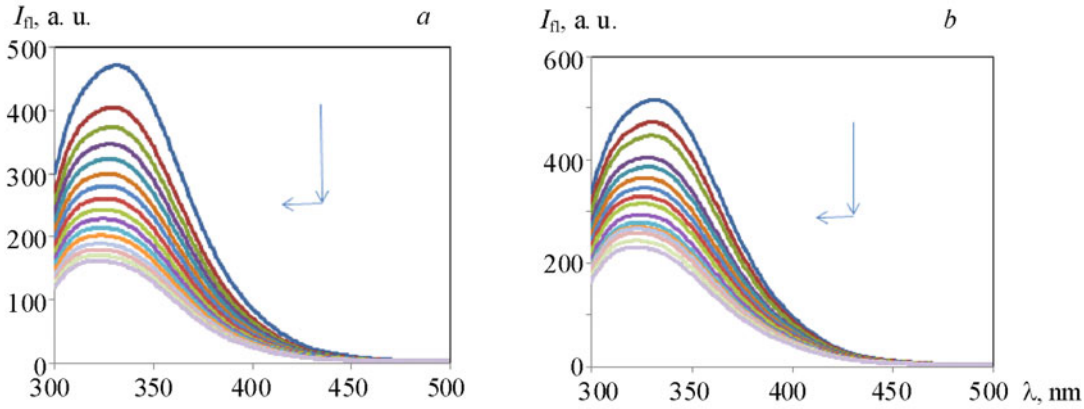

Fig. 1.The fluorescence spectra of BLG with different concentrations of (a) quercetin and (b) taxifolin at 298 K. Peaks from top to bottom denote [BLG] = 10 μM, [flavonoid] = 0, 2.0, 4.0, 6.0, 8.0, 10.0, 12.0, 14.0, 16.0, 18.0, 20.0, 22.0, 24.0, 26.0, 28.0, and 30.0 μM.

Results and Discussion. Fluorescence quenching of protein could be utilized to study drug protein binding [26]. Fluorescence quenching is due to the decrease in the quantum yield of fluorescence from the fluorophore when it interacts with a quencher molecule, which can be the result of energy transfer, ground complex formation, and dynamic quenching processes [27, 28]. BLG has two Trp residues; Trp 19, which is responsible for the main fluorescence intensity of BLG, is placed in a polar environment. The other Trp 61 with smaller less contribution to the BLG fluorescence is exposed to an aqueous environment [29, 30]. When BLG interacts with other molecules, the Trp fluorescence may change. Moreover, when the interaction between ligands and protein is investigated by fluorescence spectroscopy, some ligands absorb light at the excitation and emission wavelengths of protein, which affect the determination of fluorescence intensity. This auto absorption is called the inner filter effect. So, to remove the inner filter effects of protein and ligand, absorbance measurements were carried out at excitation and emission wavelengths of the fluorescence measurements. The fluorescence intensity was corrected using the following equation [31]:

$$F_c = F \,\text{antilog}[(A_{ex} + A_{em})/2] \,, \tag{1}$$

where F_c is the corrected fluorescence intensity, F is the intensity observed with the spectrofluorimeter, and A_{ex} and A_{em} are the absorbance values of taxifolin at the excitation and emission wavelengths, respectively. The fluorescence intensity used in this article was corrected. At the excitation wavelength of 295 nm, the fluorescence spectra of BLG as a function of the concentration of flavonoid are shown in Fig. 1. There can be seen a strong fluorescence emission peak at 335 nm attributed to tryptophan residues.

Based on Fig. 1, the fluorescence intensity of BLG gradually decreases with increasing concentration of flavonoid, which indicates the interaction between flavonoid and BLG. Additionally, we noted that there is a gradual blue shift of the maximum wavelength throughout the fluorescence spectrum of BLG as quercetin and taxifolin are added to the BLG solution, progressively. This not only suggests that the flavonoid is binding to the hydrophobic cavity in the protein but also indicates that the hydrophobicity around tryptophan residues will increase and the polarity will decrease [32]. Quenching mechanisms may be either static or dynamic. In static quenching, a ground state complex is formed between the quencher and fluorophore. Dynamic quenching occurs when the quencher diffuses to the fluorophore during the lifetime of an excited state [33]. The Stern–Volmer analysis was applied to study the BLG fluorescence quenching data [34]:

$$F_0/F = 1 + K_q\tau_0[Q] = 1 + K_{SV}[Q] \,, \tag{2}$$

where F_0 and F are the fluorescence intensities in the absence and presence of the quencher, respectively; K_q is the quenching rate constant of the biomolecule, K_{SV} is the Stern–Volmer dynamic quenching constant, τ_0 is introduced as the average lifetime of the fluorophore (in this case Trp) that has been reported for the Trp residues of BLG at neutral pH of 1.28 ns [11], and [Q] is the quencher concentration. Equation (2) was used to determine K_{SV} by adding linear regression to the plots of F_0/F against [Q]. The values of K_q for flavonoids are listed in Table 1. The obtained bimolecular quenching constants for BLG-quercetin and BLG–taxifolin complexes are 4.21×10^{13} and 3.36×10^{13} $M^{-1} \times s^{-1}$, respectively, which is higher than

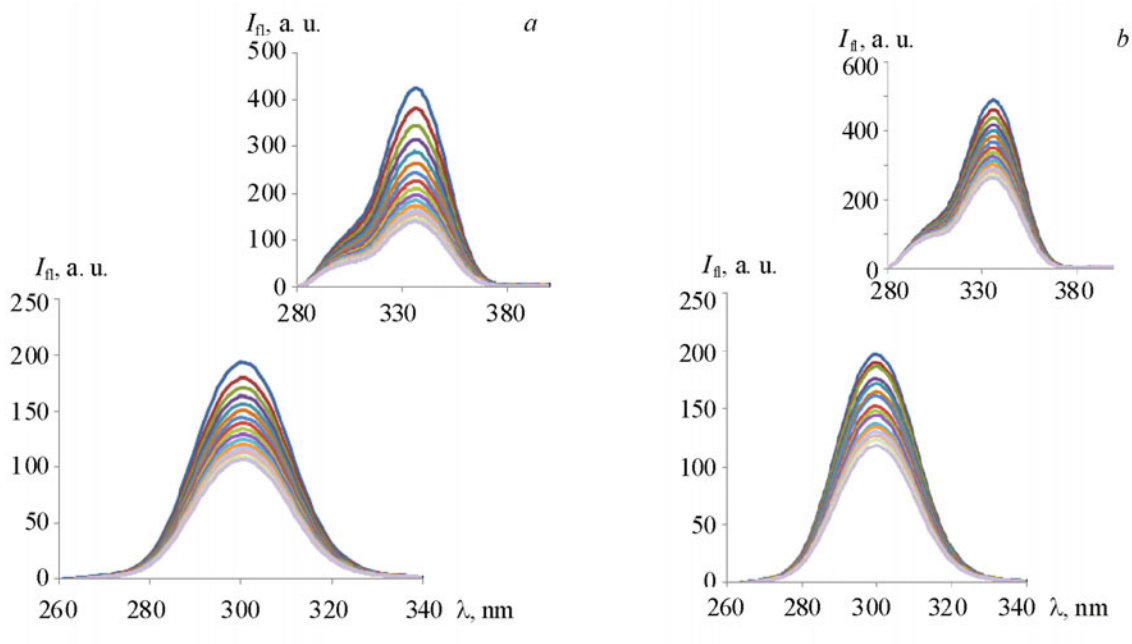

Fig. 2. Fluorescence spectrum of (a) the BLG–quercetin system at Δλ = 15 nm, inset: Δλ = 60 nm, and (b) the BLG–taxifolin system at Δλ = 15 nm, inset: Δλ = 60 nm, at 298 K.

TABLE 1. The Stern–Volmer Constants K_{SV}, Quenching Constants K_q, Binding Constants K_a, and the Number of Binding Sites n for the BLG–Flavonoid System

System	K_{SV}, M^{-1}	K_q, $M^{-1}\cdot s^{-1}$	K_a, M^{-1}	n	R^2
BLG–quercetin	5.4×10^4	4.21×10^{13}	1.14×10^5	1.15	0.991
BLG–taxifolin	4.3×10^4	3.36×10^{13}	9.03×10^4	1.07	0.995

the maximum possible value for the diffusion controlled quenching (2.0×10^{10} $M^{-1} \times s^{-1}$). This suggests that the probable quenching mechanisms for BLG–quercetin and BLG–taxifolin complexes were initiated by static, not dynamic, quenching [35].

For the static quenching, the binding constant (K_a) and the number of binding site (n) were obtained through adding regression to the plots of $[\log (F_0 - F)]/F$ versus $\log [Q]$ based on the following equation [36]:

$$[\log (F_0 - F)]/F = \log K_a + n \log [Q] . \quad (3)$$

The corresponding values of K_a and n are presented in Table 1. As listed in Table 1, the binding constant (K_a) of BLG with quercetin was calculated to be 1.14×10^5 M^{-1}, which is larger than the binding constant (K_a) of BLG with taxifolin (9.03×10^4 M^{-1}). The high K_a values indicate strong interaction between quercetin and BLG. The n values are calculated to be 1.15 and 1.07, respectively, suggesting that there is a single independent binding site in BLG with quercetin and taxifolin.

We found that quercetin exhibited higher binding affinity for BLG than taxifolin with a nonplanar C-ring. Quercetin and taxifolin are similar in structure except for a nonplanar C-ring of taxifolin. Based on the above results, the effect of steric hindrance in taxifolin may be responsible for the fact that the taxifolin exhibits weaker binding affinity than quercetin for BLG.

Synchronous fluorescence spectroscopy can be used to explore microenvironmental changes of proteins. The influence of flavonoids on the synchronous fluorescence spectra of BLG at Δλ = 15 and 60 nm is shown in Fig. 2. It can be seen that when Δλ = 15 and 60 nm, with higher concentrations of flavonoid, the fluorescence intensities of the BLG–flavonoid system decreases regularly. There is no shift of the maximum emission wavelength with Δλ = 15 and 60 nm, which implies

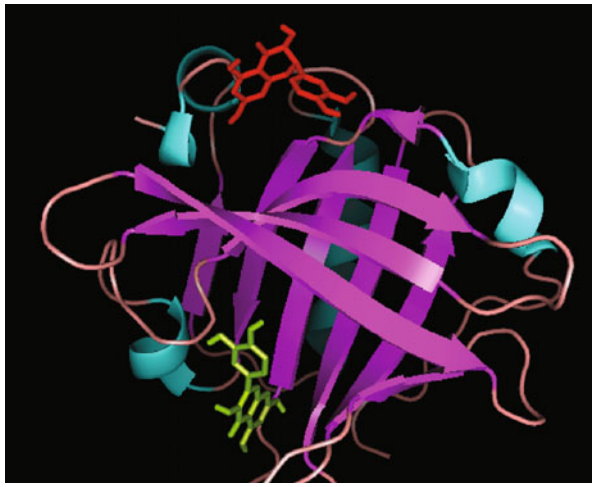

Fig. 3. Superposition of the docking poses of quercetin (green) and taxifolin (red).

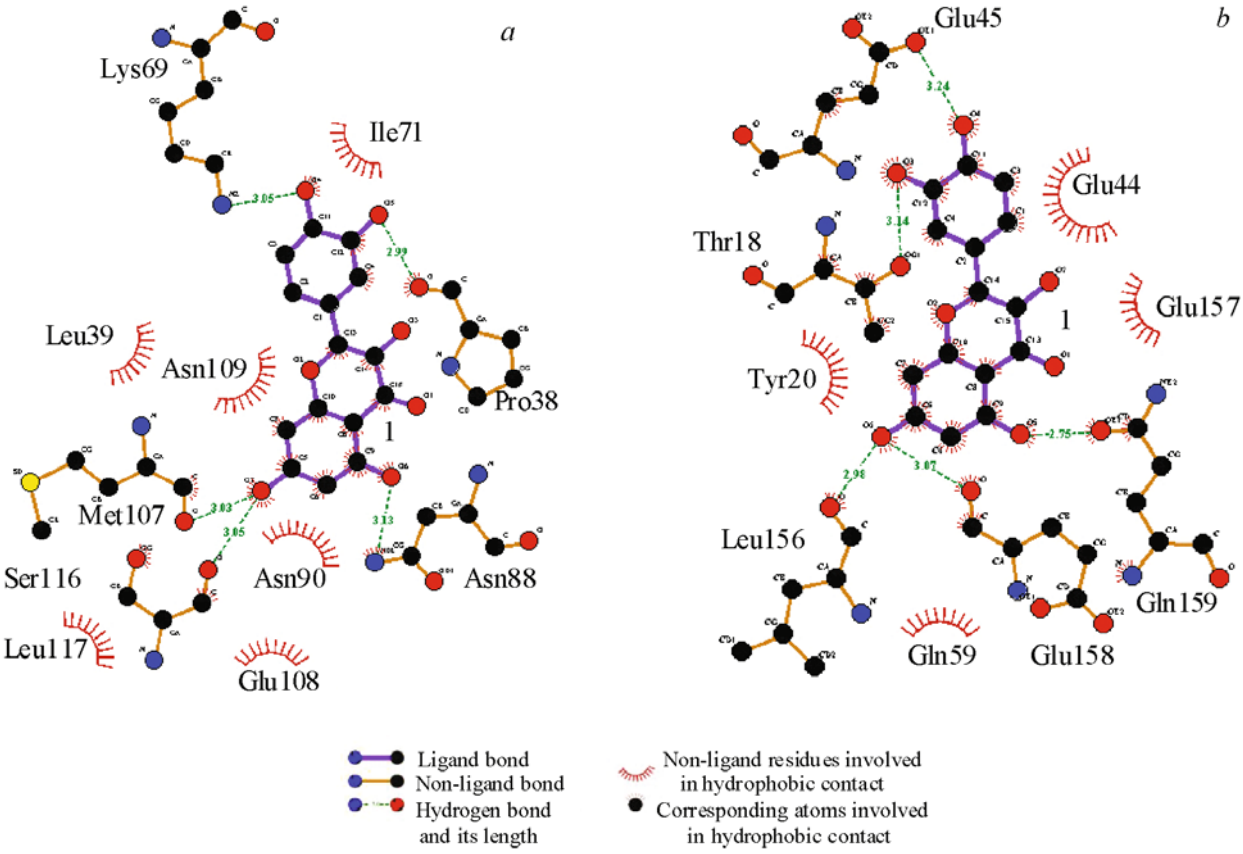

Fig. 4. The docking poses of the BLG–flavonoid complexes: (a) quercetin and (b) taxifolin. H-bonds (as highlighted by the line in green colors) are formed between flavonoids and BLG.

that the interaction of quercetin and taxifolin with BLG do not affect the conformation of the region around the Trp and Tyr residues [37].

Our spectroscopic studies were further confirmed by a molecular docking study in which quercetin and taxifolin were docked into BLG to probe the preferred binding sites of these flavonoids and their affinity towards this carrier protein (Fig. 3).

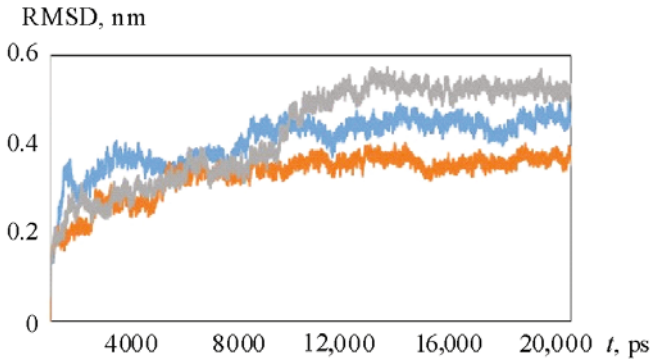

Fig. 5. Time dependence of RMSD. RMSD values for the unliganded BLG and BLG–flavonoid complexes. Unliganded BLG (gray), BLG–quercetin (blue) and BLG–taxifolin (red).

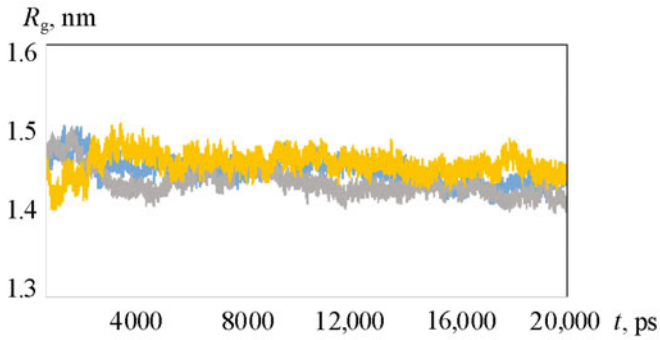

Fig. 6. Time evolution of the radius of gyration (R_g) during 20 ns of the MD simulation of BLG and the BLG–flavonoids complexes. Unliganded BLG (gray), BLG–quercetin (blue), and BLG–taxifolin (yellow).

Three potential binding sites have been reported for ligand binding to BLG: (a) the internal cavity of the β-barrel, (b) the surface hydrophobic pocket in a groove between α-helix and the β-barrel, and (c) the outer surface near Trp19–Arg124 [38]. There is a large hydrophobic cavity present in the β-barrel, and a large number of ligands may bind to this site. Prior studies on the interaction of flavonoids and BLG show that quercetin binds to this cavity [39]. The most reliable results in the docking study, based on the lowest level of energy, are shown in Fig. 4.

The internal cavity of BLG is substantially hydrophobic, and quercetin is in hydrophobic interaction with Ile(71), Leu(39), Pro(38), Asn(109), Asn(90), Glu(108), and Leu(117). In spite of the main role of hydrophobic interactions, this site concentrates on some hydrogen-bond interactions where the OH groups of quercetin interact with oxygen of Pro(38), Ser(116), Met(107) and nitrogen of Asn(88) andLys(69) (Fig. 4A). Figure 4B shows that taxifolin is in hydrophobic interaction with Glu(44), Glu(157), Gln(59), and Tyr(20). However, the OH groups of taxifolin are in hydrogen-bond interactions with oxygen of Glu(45), Thr(18), Leu(156), Glu(158), and Gln(159). According to the docking simulation, the observed free energy changes of binding (ΔG) of quercetin and taxifolin are –7.8 and –7.1 kcal/mol, respectively. These results are in agreement with spectroscopic studies and show clearly that the binding of quercetin with BLG is stronger than that of taxifolin.

Figure 5 shows that the RMSD of various systems reached equilibrium and fluctuated around the mean value. This time was about 10 ns for the unliganded BLG, BLG–quercetin, and BLG–taxifolin complexes. This evidence obviously proves that the whole system is stable and in equilibrium.

The radius of gyration (R_g) for the BLG and BLG–flavonoid complexes was also determined and plotted as a function of time to examine the protein compactness, as shown in Fig. 6. The R_g values of all systems become stable after about 5 ns, indicating that the MD simulation achieved equilibrium after 5 ns. Initially, the R_g values of the unliganded BLG and BLG–flavonoid complexes were 1.44 nm, which approved previous experimental results [40]. Also, Fig. 6 shows that the R_g

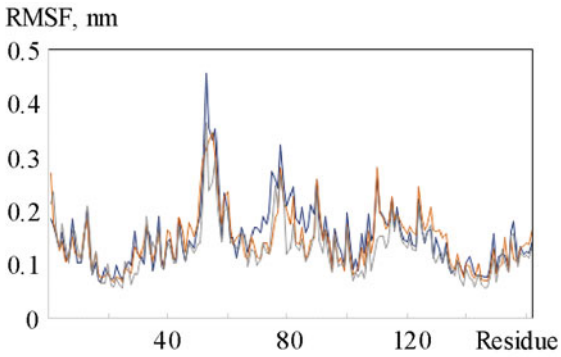

Fig. 7. The RMSF values of the unliganded BLG and BLG–flavonoids complexes were plotted against residue numbers. Unliganded BLG (dark blue), BLG–quercetin (red), and BLG–taxifolin (gray).

TABLE 2. Content of the Secondary Structural Analysis from the DSSP Method

System	α-Helix, %	β-Sheet, %	Random coil, %
Unliganded BLG	16.2	47.8	36.0
BLG–quercetin	16.7	48.1	35.2
BLG–taxifolin	17.1	47.5	35.4

value of BLG does not depend upon the complexation with flavonoids. This indicates that the environment of BLG did not change during its interaction with flavonoids.

The local mobility of protein was analyzed by calculating the time-averaged root mean square fluctuations (RMSF) of protein residues. The RMSF values versus residue numbers are illustrated in Fig. 7. The profiles of RMSF for the unliganded BLG and BLG–ligand complex were found to be similar. Furthermore, the obtained results clearly indicate that the fluctuations of residues in the internal cavity are lower than the others from, which it can be inferred that the structure of ligand binding site remains approximately rigid during the MD simulation.

The components of the secondary structure were computed based on the DSSP method to quantitatively analyze the conformational changes. The calculated secondary structure contents are presented in Table 2. The amount of the secondary structure components of the unliganded BLG and BLG–flavonoid complexes revealed that the secondary structure of BLG changed slightly upon interaction with flavonoids.

Conclusions. We have studied the binding of two kinds of flavonoids to BLG from the aspects of binding affinity and mode by fluorescence, molecular modeling, and molecular dynamics simulation techniques. Quercetin showed a BLG-binding affinity higher than that of taxifolin, which is attributed to the nonplanar C-ring and steric hindrance effect in taxifolin. The synchronous fluorescence results revealed that the microenvironment of protein did not change with addition of quercetin and taxifolin. The molecular docking results showed that quercetin and taxifolin bind in the internal cavity of BLG. The MD simulation pointed out that the RMSD of the systems reached equilibrium after 10 ns simulation time. Also, the similarity of profiles of atomic fluctuations of the BLG and BLG–flavonoid complexes suggested that the structure of the ligand binding site remained rigid during the simulation. Because pH does not have an important effect on the binding affinity of BLG [41], it can be concluded that our achieved results certified the safe transferring of these flavonoids from the stomach.

Acknowledgment. The authors are grateful to Islamic Azad University, Bandar Abbas Branch.

REFERENCES

1. D. R. Flower, A. C. North, and C. E. Sansom, *Biochim. Biophys. Acta*, 1482, 9–24 (2000).
2. S. Schlehuber and A. Skerra, *Drug Discov. Today*, 10, 23–33 (2005).
3. S. Petrovska, D. Jonkus, J. Zagorska, and I. Ciprovica, *Res. Rural Dev.*, **2**, 74–80 (2017).
4. J. C. Ioannou, A. M. Donald, and R. H. Tromp, *Food Hydrocolloid*, **46**, 216–225 (2015).

5. S. A. Forrest, R. Y. Yada, and D. Rousseau, *J. Agric. Food Chem.*, **53**, 8003–8009 (2005).
6. E. Reboul, *Nutrients*, **5**, 3563–3581 (2013).
7. S. L. Maux, S. Bouhallab, L. Giblin, A. Brodkorb, and T. Croguennec, *Dairy Sci Technol.*, **94**, 409–426 (2014).
8. T. Lefèvre and M. Subirade, *Food Hydrocolloids*, **15**, 365–376 (2001).
9. M. Sahihi, Y. Ghayeb, and A. K. Bordbar, *Spectroscopy*, **27**, 27–34 (2012).
10. L. Liang, H.A. Tajmir-Riahi, and M. Subirade, *Biomacromolecules*, **9**, 50–56 (2008).
11. L. Liang and M. Subirade, *J. Phys. Chem. B*, **114**, 6707–6712 (2010).
12. F. Mohammadi and M. Moeeni, *Mater. Sci. Eng. C*, **50**, 358–366 (2015).
13. L. A. Weston and U. Mathesius, *J. Chem. Ecol*., **39**, 283–297 (2013).
14. A. Massi, O. Bortolini, D. Ragno, T. Bernardi, G. Sacchetti, M. Tacchini, and C. D. Risi, *Molecules*, **22**, 1270–1297 (2017).
15. L. G. Costa, J. M. Garrick, P. J. Roquè, and C. Pellacani, *Oxid. Med. Cell. Longev.*, **2016**, 1–10 (2016).
16. F. S. Mohseni-Shahri, M. R. Housaindokht, M. R. Bozorgmehr, and A. A. Moosavi-Movahedi, *Can. J. Chem*., **94**, 458–469 (2016).
17. M. C. Bohin, J. P. Vincken, H. T. W. M. Van der Hijden, and H. Gruppen, *J. Agric. Food Chem.*, **60**, 4136–4143 (2012).
18. J. Essemine, I. Hasni, R. Carpentier, T. J. Thomas, and H. A. Tajmir-Riahi, *Int. J. Biol. Macromol.*, **49**, 201–209 (2011).
19. M. A. Thompson, *ArgusLab 40, Planaria Software LLC*, Seattle; http://www. ArgusLabcom
20. M. W. Schmidt, K. K. Baldridge, J. A. Boatz, S. T. Elbert, M. S. Gordon, J. H. Jensen, S. Koseki, N. Matsunaga, K. A. Nguyen, and S. Su, *J. Comput. Chem.*, **14**, 1347–1363 (1993).
21. H. J. Berendsen, D. van der Spoel, and R. van Drunen, *Comput. Phys. Commun*., **91**, 43–56 (1995).
22. A. W. SchuÈttelkopf and D. M. Van Aalten, *Acta Crystallogr. D*, **60**, 1355–1363 (2004).
23. H. J. C. Berendsen, J. P. M. Postma, W. F. Van Gunstetren, and J. Hermans, *Intermolecular Forces, Interaction Models for Water in Relation to Protein Hydration*, Reidel Publishing, Dordrecht, The Netherlands (1981).
24. H. J. C. Berendsen, J. P. M. Postma, W. F. Van Gunsteren, A. DiNola, and J. R. Haak, *J. Chem. Phys.*, **81**, 3684–3690 (1984).
25. C. Danciulescu, B. Nick, and F. J. Wortmann, *Biomacromolecules*, **5**, 2165–2175 (2004).
26. M. R. Eftink and C. A. Ghiron, *Biochemistry*, **15**, 672–680 (1976).
27. M. Bhattacharyya, U. Chaudhuri, and R. K. Poddar, *Biochem. Biophys. Res. Commun*., **167**, 1146–1153 (1990).
28. J. R. Lakowicz, *Principles of Fluorescence Spectroscopy*, University of Maryland School of Medicine, 3rd ed., Springer, New York (2006).
29. C. Kanakis, P. Tarantilis, M. Polissiou, and H. A. Tajmir-Riahi, *J. Biomol. Struct. Dyn*., **31**, 1455–1466 (2012).
30. N. Tayeh, T. Rungassamy, and J. R. Albani, *J. Pharm. Biomed. Anal*., **50**, 107–116 (2009).
31. J. R. Lackowicz, *Principles of Fluorescence Spectroscopy*, Plenum Press, New York, 111–150 (1983).
32. A. Mallick, S. Maiti, B. Haldar, P. Purkayastha, and N. Chattopadhyaya, *Chem. Phys. Lett.*, **371**, 688–693 (2003).
33. P. Bourassa, S. Dubeau, G. M. Maharvi, A. H. Fauq, T. Thomas, and H. A. Tajmir-Riahi, *Biochimie*, **93**, 1089–1101 (2011).
34. F. Moeinpour, F. S. Mohseni-Shahri, B. Malaekeh-Nikouei, and H. Nassirli, *Chem. Biol. Interact.,* **257**, 4–13 (2016).
35. S. Deepa and A. K. Mishra, *J. Pharm. Biomed. Anal.*, **38**, 556–563 (2005).
36. J. Kang, Y. Liu, and M. Xie, *Biochim. Biophys. Acta*, **1674**, 205–214 (2004).
37. Y. Q. Wang, H. M. Zhang, G. C. Zhang, Q. H. Zhou, Z. H. Fei, Z. T. Liu, and Z. X. Li, *J. Mol. Struct.*, **886**, 77–84 (2008).
38. S. Roufik, S. F. Gauthier, X. J. Leng, and S. L. Turgeon, *Biomacromolecules*, **7**, 419–426 (2006).
39. M. Sahihi, Z. Heidari-Koholi, and A. K. Bordbar, *J. Macromol. Sci. B: Phys.*, **51**, 2311–2323 (2015).
40. D. Renard, *Small Angle Neutron Scattering Study of Protein-Polysaccharide Mixtures Undershear*, Dissertation thesis Universit´ e de Nantes, France (1994).
41. L. H. Riihimäki, M. J. Vainio, J. M. Heikura, K. H. Valkonen, V. T. Virtanen, and P. M. Vuorela, *J. Agric. Food Chem*., **56**, 7721–7729 (2008).